Journal of Membrane Science 409–410 (2012) 232–241

Contents lists available at SciVerse ScienceDirect

Journal of Membrane Science

journal homepage: www.elsevier.com/locate/memsci

Gas permeability, diffusivity, and free volume of thermally rearranged polymers based on 3,3′-dihydroxy-4,4′-diamino-biphenyl (HAB) and 2,2′-bis-(3,4-dicarboxyphenyl) hexafluoropropane dianhydride (6FDA)

David F. Sanders[a], Zachary P. Smith[a], Cláudio P. Ribeiro Jr.[a,1], Ruilan Guo[b], James E. McGrath[c], Donald R. Paul[a], Benny D. Freeman[a,*]

[a] University of Texas at Austin, Center for Energy and Environmental Resources, Department of Chemical Engineering, and Texas Materials Institute 10100 Burnet Road, Building 133, Austin, TX 78758, United States
[b] University of Notre Dame, Department of Chemical and Biomolecular Engineering, Notre Dame, IN 46556, United States
[c] Virginia Polytechnic Institute and State University, Macromolecules and Interfaces Institute and Department of Chemistry, Blacksburg, VA 24061, United States

ARTICLE INFO

Article history:
Received 11 January 2012
Received in revised form 21 March 2012
Accepted 23 March 2012
Available online 2 April 2012

Keywords:
Gas separations
Thermally rearranged
TR, HAB
6FDA
Polybenzoxazole

ABSTRACT

HAB-6FDA polyimide was synthesized from 3,3′-dihydroxy-4,4′-diamino-biphenyl (HAB) and 2,2′-bis-(3,4-dicarboxyphenyl) hexafluoropropane dianhydride (6FDA) by a two-step polycondensation method with chemical imidization. This polyimide was used as the precursor to prepare thermally rearranged (TR) polymers. The rearrangement reaction was performed at temperatures from 350 to 450 °C. Based on mass loss during the TR process, TR conversion levels as high as 76% were observed. CO_2 permeability increased from 12 Barrer in the precursor polyimide (HAB-6FDA) to 410 Barrer in the TR polymer prepared at 450 °C, while pure gas CO_2/CH_4 selectivity decreased from 42 to 24. Both diffusivity and solubility increased following the rearrangement process, but the change in gas diffusivity was the largest contribution to the increase in permeability. From the polyimide to the sample heated at 450 for 30 min, CO_2 diffusivity increased by approximately a factor of 20 while solubility increased by a factor of 1.7. Similar changes were observed for other gases. Fractional free volume increased from 15% in the polyimide precursor to 20% in the TR polymer rearranged at 450 °C. The HAB-6FDA TR polymers exhibited higher CO_2 permeability than other classes of polymers with similar free volume, suggesting a free volume distribution in these TR polymers that favors high permeability.

1. Introduction

In 2008, nearly 100 trillion scf (standard cubic feet) of natural gas were produced world wide, making natural gas processing the world's largest industrial gas separation [1]. Carbon dioxide is a key contaminant, with nearly 20% of natural gas needing CO_2 removal to meet pipeline standards [1]. Currently, amine absorption is the dominant technology for removing acid gases, such as CO_2, from natural gas [1]. However, polymer membranes are also used in this application, and membranes could play an even greater role if membrane materials with more desirable property profiles were available [1].

Recently, thermally rearranged (TR) polymers have been shown to have interesting combinations of permeability, selectivity, and chemical resistance for CO_2 removal from natural gas [2]. More specifically, early studies on this class of polymers reported high permeabilities and selectivities (e.g., CO_2 permeability coefficients of 1610 Barrer and CO_2/CH_4 selectivity values of 48) relative to conventional polymer membranes [2]. These high permeability and selectivity values have been attributed to the formation of a desirable free volume element distribution during the thermal rearrangement process [3,4]. Additionally, TR polymers appear to be resistant to CO_2-induced plasticization, which may be of interest for purifying natural gas streams containing high levels of CO_2 [2].

TR polymers are often insoluble, possibly crosslinked materials, which can make it impossible to prepare adequately thin membranes via traditional solution-based routes [2,5]. However, the polyimide precursors are typically soluble in organic solvents, which permits harnessing conventional membrane fabrication processes to prepare, for example, hollow fibers, which can be subsequently thermally rearranged to form TR polymer membranes [2].

Investigation of gas transport properties of these thermally rearranged polymers is ongoing [3,6–8]. Most prior work focused

* Corresponding author. Tel.: +1 512 232 2803; fax: +1 512 232 2807.
E-mail address: freeman@che.utexas.edu (B.D. Freeman).
[1] Current address: Celanese Ltd., Acetyl Intermediates R&D, 9502 Bayport Blvd., Pasadena, TX 77507, United States.

0376-7388/$ – see front matter © 2012 Elsevier B.V. All rights reserved.
http://dx.doi.org/10.1016/j.memsci.2012.03.060

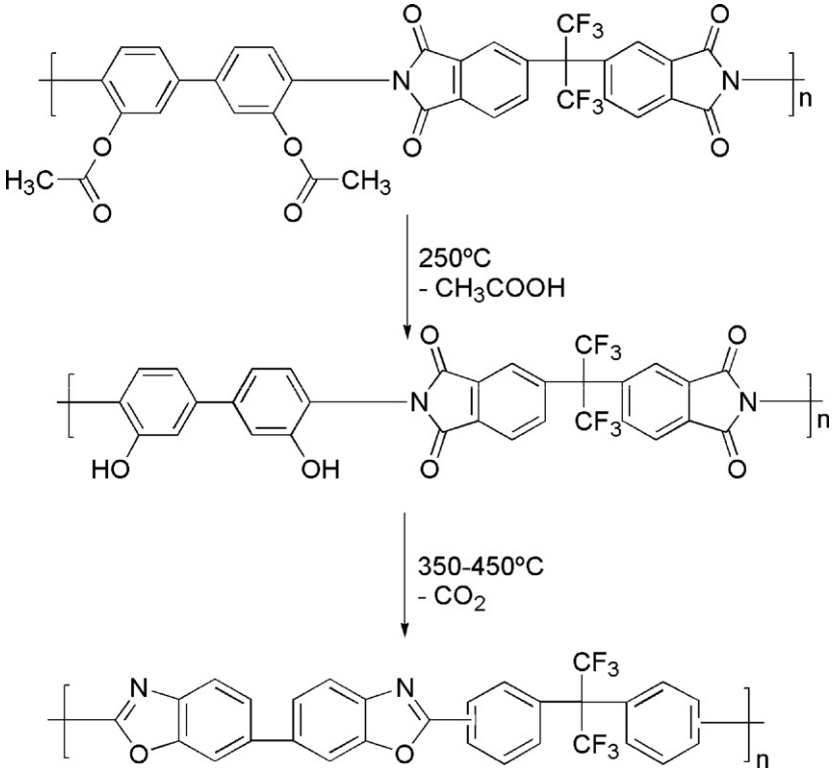

Fig. 1. Chemical structure of HAB-6FDA polyimide and its corresponding polybenzoxazole after thermal rearrangement. The mass loss due to complete rearrangement of the polyimide precursor to the final polybenzoxazole would be 24.3 wt.%.

on understanding the influence of molecular modification of polyimide precursors on TR polymer transport properties. These modifications include changing the polymer backbone, such as adding ether linkages, making copolyimdes to be used as TR polymers, and altering the rearrangement technique to form polybenzimidazoles [9–11]. Additional studies have examined the influence of polyimide synthesis route on TR polymer transport properties [12].

In this study, physical and gas transport properties of HAB-6FDA polyimide precursor and its TR analogs have been characterized. Such measurements on this material have not been previously reported. Relevant chemical structures are presented in Fig. 1. The TR process shown in Fig. 1 assumes intramolecular conversion of the aromatic polyimide precursor (API) to the thermally rearranged polybenzoxazole (PBO). If intermolecular thermal rearrangement also occurs along with the intramolecular conversion, then a network structure would be formed. Pure gas permeability coefficients of H_2, CO_2, O_2, N_2, and CH_4 are reported at 35 °C for feed pressures up to 16 atm. Gas sorption values are reported elsewhere [13], and they, along with the permeation results, were used to estimate diffusivity values to explore the solubility and diffusivity contributions to the large increases in permeability observed following thermal rearrangement. To assess free volume, several techniques have been used to measure density in these materials. The density values obtained by these methods and the subsequent estimation of free volume based on those density values are also discussed.

2. Experimental

2.1. Polymer synthesis

The polyimide based on HAB (3,3′-dihydroxy-4,4′-diaminobiphenyl) and 6FDA (2,2′-bis-(3,4-dicarboxyphenyl) hexafluoropropane dianhydride) was synthesized by chemically imidizing a poly(amic acid) precursor [13]. Monomers, purchased from Chriskev Company (Lenexa, KS, USA), were dried in a vacuum oven before use. The HAB powder was dried, in the absence of light, under vacuum at 50 °C overnight. The 6FDA powder was placed under vacuum for approximately 30 min at room temperature and then exposed to dry air at atmospheric pressure. The 6FDA was then heated at 200 °C under −10 mmHg vacuum for 6 h and finally at 120 °C under full vacuum overnight. For a typical synthesis, 20 mmol of HAB was added to 44 ml of distilled NMP and stirred with a mechanical stirrer until the diamine dissolved completely (approximately 1 h). 20 mmol of 6FDA was then added and the resulting mixture was cooled to 0 °C and stirred for roughly 12 h to form the poly(amic acid).

Chemical imidization is a common method to convert poly(amic acids) to polyimides [14,15]. In this study, chemical imidization was performed as described previously [13]. The viscous solution resulting from the poly(amic acid) synthesis was precipitated in methanol and dried in a vacuum oven at 100 °C for 1 day, then 120 °C for one day and finally 200 °C for 2 days to yield the final polyimide product. The polyimide structure was confirmed by FT-IR and ^{1}H NMR [13].

2.2. Film casting

Polymer films having thicknesses between 30 and 50 μm were cast from *N*,*N*-dimethylacetamide (DMAc) solutions of approximately 3 wt% solids. Solutions were filtered through a 5 μm polytetrafluoroethylene filter and cast onto a flat glass plate with a glass ring attached. Film thickness was controlled by the concentration of the solution and the amount of solution added to the casting ring. Films were dried at 80 °C overnight in ambient atmosphere to remove the bulk of the solvent and then at 200 °C under vacuum overnight to remove residual DMAc. Solvent removal was confirmed using thermogravimetric analysis.

2.3. Gas permeation measurements

Gas permeability coefficients of CH_4, H_2, N_2, O_2, and CO_2 were measured using a constant volume, variable pressure method [16]. The above gases are listed in order of testing. The upstream pressure in the system was measured using a STJE 1000 psig pressure transducer (Honeywell Sensotec, Columbus, Ohio, USA). The film to be studied was mounted in a 47 mm HP Filter Holder (Millipore, Billerica, MA, USA). Membranes were masked with aluminum tape and sealed with epoxy (Devcon, No. 145250, Danvers, MA, USA) to provide a well-defined area. The downstream pressure was kept below 10 Torr using a vacuum pump, and it was measured using a Baratron 626A 10 Torr capacitance manometer (MKS, Andover, MA, USA). All data were recorded using National Instruments LabVIEW Software. Pure gas permeability coefficients were measured at feed pressures ranging from approximately 3 to 16 atm. All measurements were made at 35 °C with UHP grade gases from Airgas (Radnor, PA, USA).

2.4. Thermogravimetric analysis

Thermogravimetric analysis (TGA) was performed using a TA Instruments Q500 (Newcastle, DE, USA). A nitrogen purge (40 ml/min balance, 60 ml/min sample) was used to maintain an inert atmosphere during the TGA experiments. Mass spectrometry results on these samples are reported separately [13].

2.5. Thermal rearrangement

Thermal rearrangement of film samples was performed at ambient pressure in a Carbolite Split-Tube Furnace (Carbolite, Watertown, WI, USA). A film sample, approximately 13 cm^2 in area, was placed between two ceramic plates separated by a stainless steel washer to allow the films to contract, but not curl, during thermal rearrangement. A nitrogen purge of 900 ml/min was used to maintain an inert atmosphere around the sample during thermal rearrangement. All thermal rearrangements in this study were performed by heating a sample, initially at ambient conditions, at a ramp rate of 5 °C/min to 300 °C, where the sample was held isothermally for 1 h to ensure complete imidization [17]. As will be discussed later, some loss of acetate functionality also occurs during this hold. Then, temperature was increased at 5 °C/min to the target thermal rearrangement temperature (350, 400, or 450 °C), where the sample was held for the desired amount of time (typically 30 min or 1 h in this study). The furnace was then cooled to ambient conditions at a rate no greater than 10 °C/min. This protocol was used to expose the samples to thermal histories similar to those reported in previous studies of TR polymers [2,3]. Thermal rearrangement, which occurs with a substantial loss in mass of the sample, resulted in some shrinkage of the polymer film, but the resulting films were not cracked or curled and were suitable for subsequent transport and physical property characterization.

2.6. Density measurement

Density was measured using an Ametek Two Column Density Gradient Column (Ametek TCI Division, Largo, Florida, USA). Columns were prepared from solutions of water and calcium nitrate, and experiments were performed according to ASTM D1505-68 [18]. Three small pieces (approximately 1 cm^2) of each film were introduced into the column and allowed to equilibrate for 24 h before measurement. Density was also measured using a Mettler Toledo benchtop density gradient kit (for AX/AT/AG balances, Mettler Toledo, Greifensee, Switzerland) with *n*-heptane as the reference fluid. This fluid was chosen because all four samples considered in this study exhibited very low *n*-heptane uptakes over the time scale of the density measurement.

3. Results and discussion

3.1. Thermal rearrangement

The thermal treatment conditions for samples used in gas permeability and density studies were established by first characterizing the thermal rearrangement process via TGA. The thermal profile used in the TGA studies and results for several samples are presented in Fig. 2. To mimic the thermal history applied to samples in the split tube furnace, samples in the TGA were heated from ambient conditions to 300 °C at a ramp rate of 5 °C/min, and then the sample was held at 300 °C for 1 h. This procedure ensures complete imidization of the sample before rearrangement [17]. Afterwards, temperature was increased to the desired thermal rearrangement temperature, T_2 (350, 400, 425, or 450 °C), at a ramp rate of 5 °C/min. Then, the sample was held isothermally at the desired

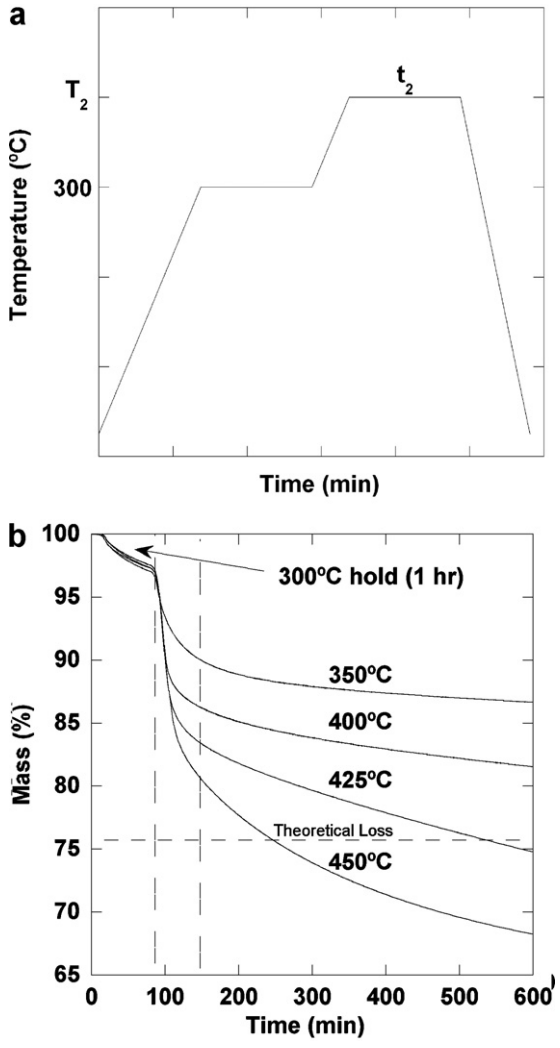

Fig. 2. (a) Heating protocol for thermal rearrangement. (b) Mass loss during the thermal rearrangement protocol for HAB-6FDA polymers using the TGA where t_2 = 10 h and T_2 is labeled on the corresponding curve. Time = 0 is selected to be when T = 200 °C. Vertical lines separate regions of acetate loss (*X*), thermal rearrangement (*Y*), and thermal degradation (*Z*). The dashed line labeled "theoretical mass loss" corresponds to the mass loss expected if the thermal rearrangement occurs as indicated in Fig. 1.

thermal rearrangement temperature, T_2, for 10 h (i.e., t_2 = 10 h in Fig. 2(a)).

Three features in Fig. 2 provide information regarding the thermal rearrangement of HAB-6FDA. The first region, below approximately 95 min (labeled "X" in Fig. 2(b)), shows a slight mass loss during the 300 °C hold. This mass loss is attributed to conversion of some of the ortho-position acetate groups to hydroxyl functionality, as shown in Fig. 1, which is believed to be the precursor to the ultimate conversion of the ortho-position hydroxyl groups to the final PBO structure shown in Fig. 1 [13]. This conversion is believed to take place due to the presence of trace amounts of water in the polymer. The acetic acid byproduct has been observed via ^{1}H NMR, and further details regarding this mechanism are reported elsewhere [19]. The second region (labeled "Y" in Fig. 2(b)), at times longer than approximately 95 min, contains a substantial mass loss ascribed to thermal rearrangement of the ortho-functional polyimide to the associated PBO (cf., Fig. 1) [2,20,21]. The magnitude of this mass loss depends on rearrangement temperature. The third region (labeled "Z" in Fig. 2(b)), at times beyond approximately 150 min, shows a continuous, approximately linear mass loss that is more rapid at higher temperatures. This mass loss is believed to mark, at least in part, the onset of thermal degradation of the polymer when held for long periods of time at high temperatures. At treatment temperatures of 425 and 450 °C, the mass loss increases beyond the value expected if thermal rearrangement were the only mechanism for mass loss, so we assume that thermal degradation must occur either following or alongside thermal rearrangement at these temperatures. The resulting films were brittle, which we have taken as an indication that the polymer was undergoing thermal degradation. The maximum mass loss labeled in the figure ("Theoretical Mass Loss"), which is 24.3%, corresponds to the mass loss associated with complete conversion of the starting polymer to the final polybenzoxazole structure as indicated in Fig. 1. Long heat treatment times, even at lower thermal treatment temperatures of 350 and 400 °C, which do not result in mass losses beyond that expected for complete thermal rearrangement (i.e., toward the right hand side of region "Z" in Fig. 2(b)), also result in brittle films, which we speculate further supports the hypothesis that at least some thermal degradation is occurring. However, we cannot rule out the possibility that further rearrangement at these temperatures may also be contributing to the decrease in mechanical properties in these films.

Based upon this TGA screening study, thermal treatment protocols were selected to ensure that samples used for permeation and density studies experienced minimal thermal degradation. In these cases, samples large enough for permeation and density measurements were thermally rearranged in a split-tube furnace. The time that the samples were held at the desired rearrangement temperature was selected to be shortly after the rapid mass loss associated with thermal rearrangement, between approximately 100 and 150 min in Fig. 2b, to minimize thermal degradation. The filled circles in Fig. 3 denote the times chosen for thermal treatment at the desired rearrangement temperature for rearrangement temperatures of 350 (1 h), 400 (1 h), and 450 °C (30 min). These protocols were selected so that transport property changes would be due principally to thermal rearrangement and not due to polymer degradation. The mass loss results were used to estimate the conversion of the polyimide precursor to the final PBO TR structure because, if there is no significant thermal degradation, all mass loss should be due to thermal rearrangement. In this regard, Eq. (1) was used to estimate the percent conversion of the polyimide precursor to TR polymer:

$$\%\,\text{Conversion} = \frac{\text{Actual Mass Loss}}{\text{Theoretical Mass Loss}} \times 100 \qquad (1)$$

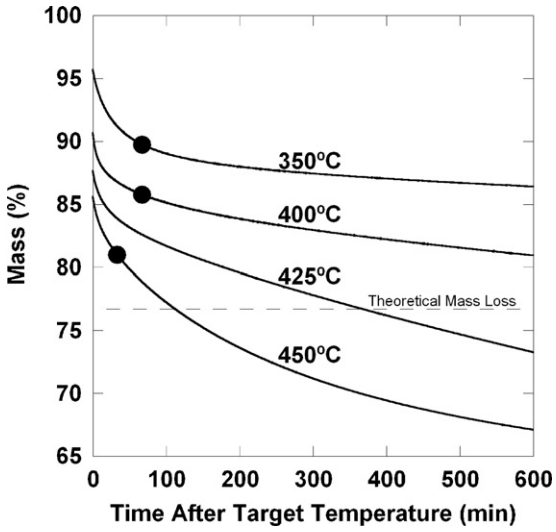

Fig. 3. TGA thermograms showing mass loss as a function of time that the sample was held at the rearrangement target temperature, T_2. Values of T_2 are given in the figure. Samples prepared at the conditions indicated by the filled circles were used for transport property characterization.

Table 1
Percent conversion of samples used to characterize HAB-6FDA TR polymer transport properties.

Treatment temperature (°C)	Treatment time (min)	Conversion (%)
–	–	0
350	60	39
400	60	60
450	30	76

Using Eq. (1) and the TGA results, conversion was estimated for polymer films after undergoing the thermal treatments selected from TGA experiments, and the resulting values are recorded in Table 1. Conversions range from 39% to 76% and were consistent when measured in both the TGA and the furnace. Conversions higher than 76% were not pursued to minimize thermal degradation.

The loss of the acetate group, leaving a hydroxyl group in its place, likely occurs before the resulting hydroxyl groups undergo thermal rearrangement to reach the final benzoxazole structure. This conversion can be observed by the appearance of hydroxyl peaks in FT-IR measurements after thermal conversion [13]. This measure of conversion does not distinguish between loss of the acetate group and conversion of the resulting hydroxyl groups to benzoxazole structures.

3.2. Pure gas permeability and selectivity

Pure gas permeabilities of CH_4, N_2, O_2, CO_2, and H_2 were measured at pressures ranging from 3 to 16 atm at 35 °C. Table 2 presents pure gas permeability coefficients of HAB-6FDA polyimide and its partially converted TR analogs at a feed pressure of 10 atm. Uncertainties were calculated using propagation of error [22]. As conversion increases, permeability increases. For example, CO_2 permeability increases by nearly a factor of three after treatment at 350 °C for 1 h, which corresponds to 39% conversion. After thermal rearrangement at 450 °C for 30 min, CO_2 permeability increases by more than a factor of 30. The relative increase in gas permeability is highest for methane and lowest for hydrogen. Thus, the extent of permeability increase with conversion is greater in molecules with larger kinetic diameters [23]. If a central feature of the TR conversion process is to increase average free volume,

Table 2
Pure gas permeability (Barrer) of HAB-6FDA polyimide and TR polymers at 10 atm and 35 °C.

Sample	Conversion (%)	CH_4	N_2	O_2	CO_2	H_2
HAB-6FDA	0	0.313 ± 0.007	0.56 ± 0.01	3.18 ± 0.07	12.0 ± 0.3	37.8 ± 0.9
TR350	39	0.77 ± 0.01	1.62 ± 0.03	8.9 ± 0.2	35.3 ± 0.6	95 ± 2
TR400	60	5.6 ± 0.4	8.7 ± 0.6	39 ± 3	160 ± 10	290 ± 20
TR450	76	18.2 ± 0.4	25.3 ± 0.6	100 ± 2	410 ± 10	530 ± 10

Note: uncertainties were estimated using the propagation of errors method [22].

Table 3
Pure gas selectivity of HAB-6FDA polyimide and TR polymers at 10 atm and 35 °C.

Sample	CO_2/CH_4	O_2/N_2	CO_2/N_2	H_2/N_2
Polyimide	38 ± 1	5.7 ± 0.2	21.6 ± 0.7	68 ± 2
TR350	46 ± 1	5.5 ± 0.2	21.7 ± 0.5	58 ± 2
TR400	28 ± 3	4.5 ± 0.5	18.2 ± 0.2	33 ± 3
TR450	22.4 ± 0.7	3.9 ± 0.1	16.1 ± 0.5	21.0 ± 0.6

Note: uncertainties were estimated using the propagation of errors method [22].

this trend is reasonable and consistent with previous reports on TR polymers [2].

For many separations, pure gas selectivity in TR polymers decreases as conversion increases, as reported previously by Park et al. for polymers imidized in the solid state from poly(amic acids) [3]. As shown in Table 3, the TR350 sample shows only a slight loss in gas selectivity compared to the polyimide precursor, except for CO_2/CH_4, which shows an increase in selectivity. This result may be due to a more favorable free volume distribution, which improves the separation performance of the polymer.

Figs. 4 and 5 present permeability and pure gas CO_2/CH_4 selectivity as a function of conversion of the API to its PBO. From these results, permeability becomes increasingly sensitive to conversion as conversion increases. Selectivity seems to become less sensitive to conversion at higher conversions; for example, the selectivity decreases by 35% as conversion increases from 39 to 60%, while selectivity only decreases by 17% as conversion increases from 60 to 76%. Based on this result, to achieve high permeability/selectivity combinations, it may be of interest to consider polymers that rearrange to high conversion without significant thermal degradation.

One way to determine whether permeability is simply being exchanged for selectivity in the TR conversion process is to compare the permeability and selectivity values on an upper bound plot. Fig. 6 presents Robeson's 1991 and 2008 upper bounds for CO_2/CH_4 separation [24,25]. Comparing the changes in permeability and

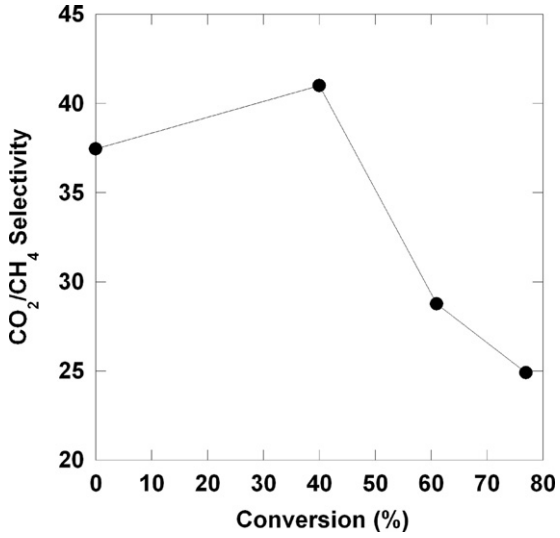

Fig. 5. CO_2/CH_4 pure gas selectivity as a function of TR conversion.

selectivity with the upper bound lines, thermal rearrangement moves gas transport properties of the HAB-6FDA polymers across the 1991 upper bound and closer to the 2008 upper bound, so thermal rearrangement improves the permeability/selectivity combinations of these materials.

As shown in Figs. 7–9, permeability was also measured at feed pressures ranging from approximately 3 to 16 atm. Permeability decreases with increasing pressure, most notably for more condensable gases such as CO_2 and CH_4. This behavior is typical for glassy polymers [26]. No plasticization behavior was observed for CO_2 up to 16 atm in these pure gas studies, and permeability decreased or was constant with increasing pressure, suggesting

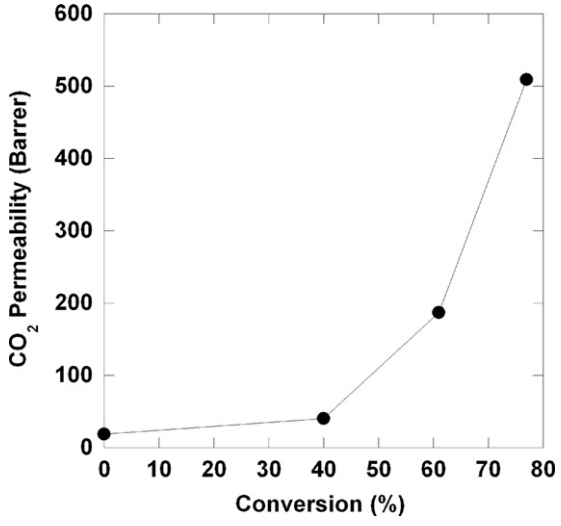

Fig. 4. CO_2 permeability as a function of TR conversion.

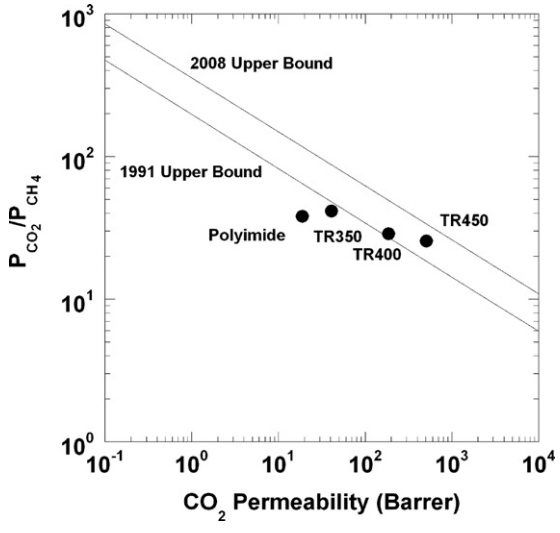

Fig. 6. Permeability/selectivity properties of HAB-6FDA polyimide and TR polymers compared with 1991 and 2008 upper bounds [24,25].

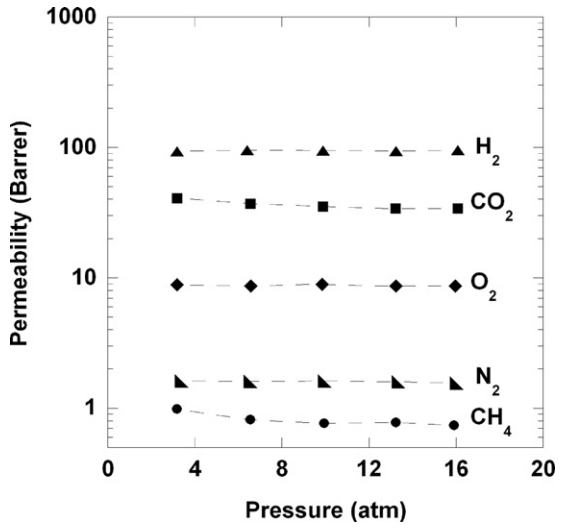

Fig. 7. Permeability as a function of feed pressure for HAB-6FDA-TR350 at 35 °C.

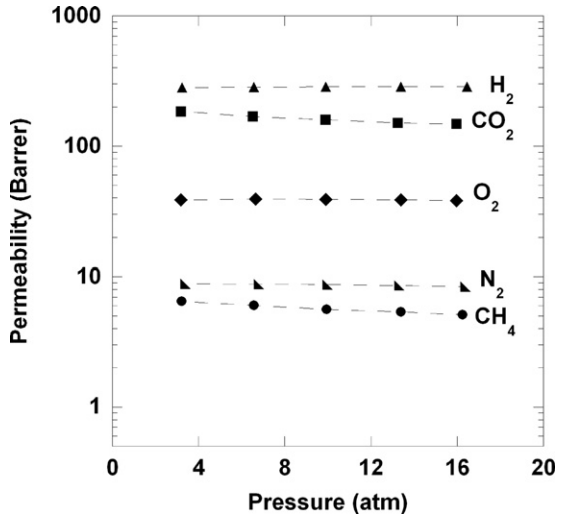

Fig. 8. Permeability as a function of feed pressure for HAB-6FDA-TR400 at 35 °C.

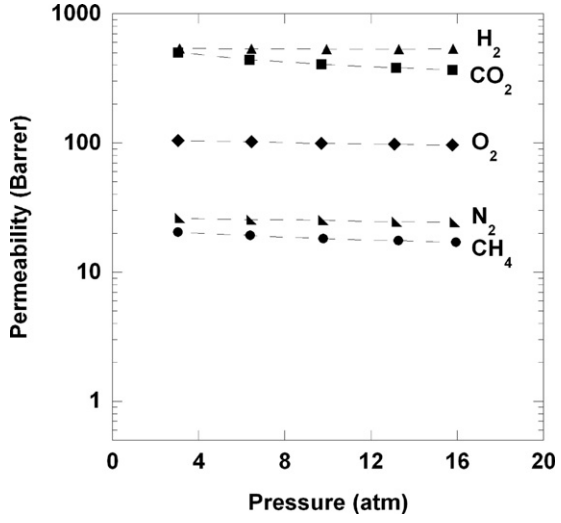

Fig. 9. Permeability as a function of feed pressure for HAB-6FDA-TR450 at 35 °C.

that no defects were introduced into the films during thermal rearrangement.

The permeabilities of HAB-6FDA TR polymers reported in this study were nearly an order of magnitude lower than those of the APAF-6FDA based TR polymers reported by Han et al., which were also synthesized using chemical imdization [12]. Polymers containing many 6F linkages typically exhibit higher gas permeabilities than other polymers, such as those containing HAB [3,27]. TR polymers explored by Han et al. were thermally rearranged at 450 °C for 1 h, which would result in some thermal degradation in the HAB-6FDA polymers used in this study. Therefore, identical heat treatment protocols were not pursued. The extent of conversion to the TR polymer was not reported by Han et al., so comparison of changes in permeability at a fixed conversion is not possible. Han et al. also measured permeability at a lower upstream pressure and temperature than used in our studies. Lower pressure increases permeability due to dual-mode effects while lower temperature commonly decreases permeability in polymers due to restricted chain motion. These differences in measurement conditions also make a quantitative comparison of permeabilities difficult.

3.3. Permeability, diffusivity, and solubility

Permeability in dense polymer films can be described by the solution-diffusion model as shown in Eq. (2) [28]:

$$P = D \times S \tag{2}$$

where P is the gas permeability, D is the diffusion coefficient, S is the solubility coefficient, and all are typically dependant on pressure in glassy polymer such as those considered in this study [13].

The permeability of HAB-6FDA polyimide and its corresponding TR polymers was measured, and, using solubility coefficients reported elsewhere [13], diffusivity values were calculated using Eq. (2). Table 4 presents representative P, D and S values for CH_4, N_2, O_2, CO_2, and H_2 at 10 atm and 35 °C. The increase in diffusivity with conversion is the dominant contribution to the observed increase in gas permeability. Solubility also increases as conversion increases, but not to the same extent as diffusion coefficients. For example, diffusivity for all gases increases by approximately an order of magnitude, while solubility typically increases by approximately a factor of approximately two as conversion increases from 0 to 76%.

Table 5 compares P, D, and S values for CO_2 of the HAB-6FDA series of polymers with values from Matrimid® and cellulose acetate, materials similar to those used commercially for natural gas separation [1,29–31]. HAB-6FDA exhibits much higher CO_2 permeabilities after thermal rearrangement while maintaining good CO_2/CH_4 selectivity values. For example, the HAB-6FDA-TR400 sample has a CO_2 permeability of 160 Barrer compared to 10 and 4.8 Barrer for Matrimid® and cellulose acetate, respectively. The CO_2/CH_4 selectivity is comparable for all samples, with the Matrimid® polyimide having the highest selectivity at 35, cellulose acetate following at 32, and the HAB-6FDA-TR400 sample having a selectivity of 29. The permeability and selectivity values of TR polymer are tunable by thermal treatment temperature and time. The TR350 sample has a selectivity of 45, higher than that of either Matrimid® or cellulose acetate polymers, and it has a CO_2 permeability of approximately 35.3 Barrer, more than three times higher than that of Matrimid® polyimide and approximately 6 times higher than that of cellulose acetate.

The changes in selectivity as conversion increases can also be interpreted within the framework of the solution-diffusion model. Because permeability depends upon solubility and diffusivity, permeability selectivity can be separated into solubility selectivity and diffusivity selectivity. Table 6 presents pure gas diffusivity and solubility selectivity for CO_2/CH_4 at 35 °C and 10 atm. From these

Table 4
Permeability, diffusivity, and solubility for HAB-6FDA polyimide and TR polymers at 10 atm at 35 °C.

Gas	Sample	Permeability (Barrer)	Solubility (cm^3 (STP)/(cm^3 polymer atm) [13]	Diffusivity × 10^9 (cm^2/s)
CH_4	Polyimide	0.313 ± 0.007	1.07 ± 0.08	2.2 ± 0.2
	TR 350	0.77 ± 0.01	1.65 ± 0.09	3.5 ± 0.2
	TR 400	5.6 ± 0.4	2.6 ± 0.1	17 ± 1
	TR 450	18.2 ± 0.4	2.8 ± 0.1	50 ± 2
N_2	Polyimide	0.56 ± 0.01	0.44 ± 0.08	10 ± 2
	TR 350	1.62 ± 0.03	0.69 ± 0.08	18 ± 2
	TR 400	8.7 ± 0.6	1.11 ± 0.09	60 ± 6
	TR 450	25.3 ± 0.6	1.18 ± 0.09	160 ± 10
O_2	Polyimide	3.18 ± 0.07	0.60 ± 0.08	40 ± 5
	TR 350	8.9 ± 0.2	0.94 ± 0.08	72 ± 6
	TR 400	39 ± 3	1.42 ± 0.09	210 ± 20
	TR 450	100 ± 2	1.52 ± 0.09	500 ± 30
CO_2	Polyimide	12.0 ± 0.3	4.04 ± 0.09	22.6 ± 0.8
	TR 350	35.3 ± 0.6	5.18 ± 0.09	52 ± 1
	TR 400	160 ± 10	6.7 ± 0.1	180 ± 10
	TR 450	410 ± 10	7.0 ± 0.1	440 ± 10
H_2	Polyimide	37.8 ± 0.9	0.21 ± 0.07	1400 ± 400
	TR 350	95 ± 2	0.25 ± 0.07	2800 ± 900
	TR 400	290 ± 20	0.35 ± 0.09	6000 ± 2000
	TR 450	530 ± 10	0.35 ± 0.08	11,000 ± 3000

Note: uncertainties were estimated using the propagation of errors method [22].

Table 5
Permeability, diffusivity, and solubility coefficients of HAB-6FDA polyimide and TR polymers compared to common polymers used in natural gas separations. Data are reported at 10 atm and 35 °C unless otherwise noted.

Sample	P_{CO_2} [Barrer]	P_{CO_2}/P_{CH_4}	$D_{CO_2} \times 10^9$ (cm^2/s)	S (cm^3 gas(STP)/(cm^3 polymer (atm)) [13]
Matrimid® Polyimide[a]	10	36	42	1.8
Cellulose acetate[b]	4.8	32	77	0.46
Polyimide	12	40	23	4.05
TR350	35.3	45	52	5.18
TR400	160	29	180	6.7
TR450	410	24	440	7.0

[a] *P* from Vu et al. [31]; *S* from Moore and Koros [29] at 3 atm.
[b] Data from Puleo et al. [30] at 1 atm.

results, solubility selectivity decreases as thermal treatment temperature increases, but diffusivity selectivity reaches a maximum at a treatment temperature of 350 °C. This maximum in selectivity may reflect a more favorable cavity size and free volume distribution for this gas pair. Table 6 also shows the solubility and diffusivity selectivities of Matrimid® and cellulose acetate polymers. In general, the HAB-6FDA-TR polymers show lower solubility selectivities and higher diffusivity selectivities than Matrimid® and cellulose acetate polymers, so these TR polymers are more effective at separating gases based on size, but less effective at separating based on solubility differences.

Table 7 shows that a maximum in CO_2/CH_4 selectivity occurs for the TR350 sample. This maximum also occurs for all gas pairs containing methane, but for gas pairs not including methane, no maximum is observed. These data suggest that the cavity size and free volume distribution in these TR polymers are favorable for separations involving methane. As expected, the selectivities shown in Table 7 are also highest for gas pairs with the largest difference in kinetic diameter. For higher treatment temperatures, such as 450 °C, both diffusivity and solubility selectivities are approximately 25% lower than in HAB-6FDA polyimide, so decreases in permeability selectivity are due to diffusivity and solubility increasing more for CH_4 as a function of conversion than for CO_2.

Table 6
CO_2/CH_4 diffusivity and solubility selectivity of HAB-6FDA polyimide and TR polymers. Data are reported at 10 atm and 35 °C unless otherwise noted.

Sample	P_{CO_2}/P_{CH_4}	D_{CO_2}/D_{CH_4}	S_{CO_2}/S_{CH_4}
Matrimid® polyimide[a]	36	2	15.3
Cellulose acetate[b]	32	4	8.2
Polyimide	38	12	3.8
TR350	46	14	3.1
TR400	28	11	2.6
TR450	22	9	2.5

[a] *P* from Vu et al. [31], *S* from Moore and Koros [29] at 3 atm.
[b] Data from Puleo et al. [30] at 1 atm.

3.4. Fractional free volume

Fractional free volume was estimated using Eq. (3) [32]:

$$FFV = \frac{V - V_0}{V} \quad (3)$$

Table 7
Pure gas methane permeability selectivities for HAB-6FDA polyimide and TR polymers at 10 atm and 35 °C.

Sample	N_2/CH_4	O_2/CH_4	CO_2/CH_4	H_2/CH_4
Polyimide	1.77 ± 0.05	10.1 ± 0.3	38 ± 1	120 ± 4
TR350	2.11 ± 0.04	11.6 ± 0.3	46 ± 1	123 ± 3
TR400	1.6 ± 0.2	6.9 ± 0.7	28 ± 3	51 ± 5
TR450	1.39 ± 0.04	5.5 ± 0.2	22.4 ± 0.7	29.3 ± 0.8

Note: uncertainties were estimated using the propagation of errors method [22].

Table 8
Density of HAB-6FDA polyimide and TR polymer density using density gradient column without corrections for water uptake.

Sample	Density (g/cm^3)
Polyimide	1.4255 ± 0.0004
TR350	1.4404 ± 0.0002
TR400	1.4010 ± 0.0003
TR450	1.3586 ± 0.0002

Note: uncertainties were calculated as the standard deviation of at least three repeat measurements.

where V_O is the so-called occupied volume of the polymer chains [33,34]. V is the specific volume, which is the inverse of the density of the polymer. V_O is determined using a group contribution method as follows:

$$V_O = 1.3 \sum V_W \quad (4)$$

where V_W is the van der Waal's volume of molecular groups comprising the polymer backbone [33,34].

Previously, density of TR polymers was measured using a density determination kit for an analytical balance [3]. In this method, based on Archimedes' principle, the polymer sample was weighed in air and in water, and the density of the polymer was inferred from the difference of the sample weight in air and in water [3]. In this study, density was measured using: (1) a density gradient column and (2) a density determination kit and an analytical balance. However, for the analytical balance method, *n*-heptane was used as the auxiliary liquid to minimize any artifacts that might arise due to water uptake by the sample. This hydrocarbon, a much larger molecule than water, was not sorbed to a measurable extent in the samples during the measurements.

Table 8 presents density values obtained using the density gradient column method. These results may be influenced by any water sorbed by the samples during the measurement, as water uptake could potentially alter the overall density of a sample. Density determination using the density kit and an analytical balance provides more flexibility in the choice of the liquid used for the measurement, and a fluid that does not interact with the polymer can be more easily chosen. However, this method is generally less precise than the density gradient column method, yielding density values accurate to approximately ±0.01 g/cm^3 rather than approximately ±0.0003 g/cm^3 in the case of the density gradient column.

The density of the TR350 sample, as measured by the density gradient column, is higher than that of the polyimide, while densities of TR polymers rearranged at higher temperatures are lower than that of the initial polyimide. This higher density measured in the column is attributed to an increased presence of hydroxyl groups from monomers that lost ortho-position acetate groups, but did not go undergo thermal rearrangement to form the final benzoxazole. The presence of these hydroxyl groups may influence the water uptake by the polymer and alter the measured density.

The equilibrium water uptake of HAB-6FDA polyimide and its TR polymers are recorded in Table 9. Both the polyimide and TR400 sample show relatively low water uptake values of 0.5%, while the TR350 and TR450 samples show much higher water uptakes of 2.9% and 2.1%, respectively. The increased water uptake in the TR350 sample is consistent with an increased number of hydroxyl groups present from the conversion of ortho-position acetate groups to ortho-position hydroxyl groups. These hydroxyl groups would make the polymer more hydrophilic and increase water uptake. As TR conversion increases further, a decrease in hydroxyl group concentration is observed by FT-IR as these groups are converted to benzoxazole structures, and free volume increases [13]. The increased free volume of the structure could assist in increasing water uptake [35].

Table 9
Equilibrium water uptake in HAB-6FDA polyimide and TR polymers.

Sample	Water uptake (% mass)
Polyimide	0.5 ± 0.2
TR350	2.9 ± 0.4
TR400	0.5 ± 0.4
TR450	2.1 ± 0.8

Note: uncertainties were calculated as the standard deviation of at least three repeat measurements.

Table 10
Densities using the density gradient column with corrections for water uptake and the density determination kit using *n*-heptane as a reference liquid.

Sample	Method	Density (g/cm^3)
Polyimide	Column	1.4211
TR350	Column	1.4176
TR400	Column	1.3968
TR450	Column	1.3422
Polyimide	Density kit	1.407 ± 0.009
TR350	Density kit	1.398 ± 0.009
TR400	Density kit	1.400 ± 0.009
TR450	Density kit	1.34 ± 0.01

Note: uncertainties were calculated as the standard deviation of at least three repeat measurements.

Two limits on the effect of water uptake on density are provided by the so-called additive volume uptake and constant volume uptake models [36]. In the additive volume uptake model, water and polymer mix according to the principle of volume additivity, with the partial molar volume of water being equal to that of pure water. In the constant volume water uptake model, water sorbs into a polymer with no change in volume. As reported by Rowe et al., polysulfone and Matrimid® polyimide each showed approximately 70% additive volume water uptake and 30% constant volume water uptake over a range of relative humidities [36]. Therefore, in this study, these proportions of additive volume and constant volume water uptake were used to correct density measurements from the density gradient column for water uptake. Using this approximation, corrected densities from the density gradient column are listed in Table 10 and shown alongside measurements made using a benchtop density measurement kit with *n*-heptane as the reference liquid. Table 10 shows that there is relatively good agreement between the two techniques after corrections are made for water uptake. Density values from the two measurement techniques are plotted against each other in Fig. 10 to give a visual comparison. This agreement suggests that the water uptake during density gradient column measurements is significant, especially in the TR350 sample, and should be accounted for in density values obtained using this method.

The occupied volume of each polymer sample was estimated using the group contribution method [33,34], modified as shown in Eq. (5) to account for partial conversion of the polyimide to the TR polymer:

$$V_O = cV_{O,TR} + (1 - c)V_{O,PI} \quad (5)$$

where $V_{O,TR}$ is the occupied volume of TR polymer chains (cm^3/g), $V_{O,PI}$ is the occupied volume of polyimide chains (cm^3/g), and c is the fractional mass conversion, calculated as the actual mass loss measured by TGA divided by the theoretical mass loss needed to achieve 100% conversion of the polyimide precursor to the TR polymer. The relevant van der Waal's volumes were obtained from the literature [33,34,37,38]. This approach requires the structure of the remaining polyimide to be known. Based on previous discussion in this work and elsewhere, the *ortho*-position acetate groups can be converted to hydroxyl groups prior to final conversion to benzoxazole structures [13]. However, we do not have a quantitative

Table 11
Fractional free volume (FFV) of HAB-6FDA polyimide and TR polymers.

Sample	Conversion (%)	FFV (%)
HAB-6FDA	0	15.0
TR350	39	15.1
TR400	60	16.3
TR450	76	19.6

estimate of the number of acetate and hydroxyl groups in partially converted samples because they become insoluble, making quantitative determination difficult. Fortuitously, the occupied volume of the acetate and hydroxyl containing polymers differ by less than 2%, so this lack of complete information regarding the structure has a negligible impact on free volume calculations. In the calculations described below, any unconverted functional groups are assumed to be acetate groups.

The calculated fractional free volume values are presented in Table 11. Qualitatively consistent with the trends observed in transport properties, fractional free volume increases from 15% in the polyimide to nearly 20% in the TR450 sample. However, the transport properties would suggest a larger increase in free volume. Fig. 11 presents CO_2 permeability coefficients as a function of fractional free volume for the HAB-6FDA polyimide and its TR polymers, several other polyimides, and a general trend for a wide range of polymers [23].

CO_2 permeability in the HAB-6FDA polyimide and its related TR polymers is more sensitive to changes in FFV, brought about by thermal rearrangement, than expected based on results for other polymers. This result qualitatively supports the finding by Park et al. that, in addition to increasing fractional free volume, thermal rearrangement changed the free volume distribution, resulting in large cavities separated by narrow necks [2]. This free volume distribution appears to be favorable for higher gas permeabilities than other families of polymers with similar fractional free volumes.

4. Conclusions

HAB-6FDA polyimide was synthesized using chemical imidization and was successfully thermally rearranged by heat treatment

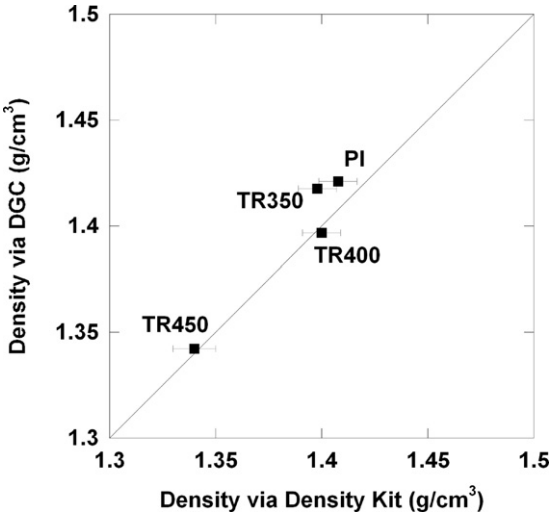

Fig. 10. Comparison of densities from the density gradient column (DGC) and density determination kit using *n*-heptane. Density values obtained using the DGC were corrected for water uptake by the method described in Rowe et al., assuming that 70% of the water uptake resulted in swelling of the polymer film via an additive mixing model and 30% of the water uptake sorbed into the polymer without changing the volume of the polymer sample [36].

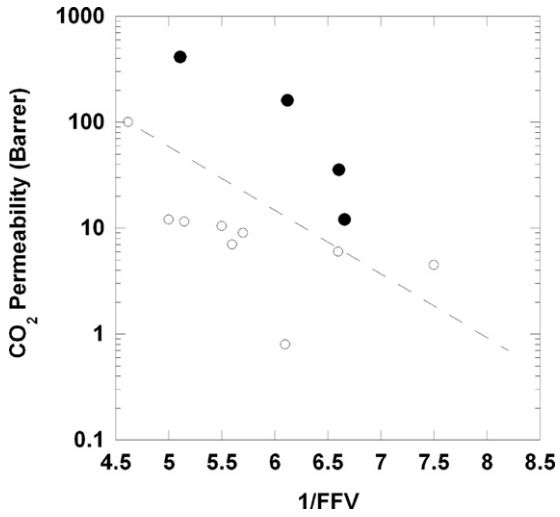

Fig. 11. CO_2 permeability at 35 °C and 10 atm feed pressure as a function of free volume for HAB-6FDA polyimide and TR polymers (filled circles) and various polyimides (open circles) [23]. The dashed line is the best fit slope for a wide range of polymers [23].

at 350 and 400 °C for 1 h and 450 °C for 0.5 h. These temperatures gave conversions of the polyimide precursor toward its TR polymer analog ranging from 39% to 76% as estimated from mass loss. Thermally rearranged polymers from HAB-6FDA had CO_2 permeabilities more than 30 times higher, at 10 atm and 35 °C, than the precursor polyimide after thermal rearrangement at 450 °C for 0.5 h. Significant increases in permeability were also observed for H_2, CH_4, N_2, and O_2. These increases in permeability with increasing conversion are due to increases in both solubility and diffusivity, although diffusivity increases were greater than solubility increases. For example, diffusivity typically increased by approximately an order of magnitude after thermal rearrangement, and solubility increased by roughly a factor of two.

Thermal rearrangement did decrease pure gas selectivity at thermal treatment temperatures above 350 °C, but thermally rearranged polymers were able to traverse the 1991 upper bound and move closer to the 2008 upper bound. Thus, thermal rearrangement improved the transport properties of these polymers and did not simply trade permeability for selectivity as might be expected for changes among a family of polymers that simply increased (or decreased) average free volume. Decreases in CO_2/CH_4 permeability selectivity were due to a decrease in both solubility and diffusivity selectivity. For example, from the polyimide to the TR450 sample CO_2/CH_4 selectivity decreased by 42%. This decrease was due to a 25% decrease in diffusivity selectivity and a 34% decrease in solubility selectivity.

Density measurements were made using both a density gradient column and a density determination kit. Water uptake measurably altered density values obtained using the density gradient column, and a correction was applied to the data to account for water uptake. Fractional free volume increased from about 15% for the polyimide to 20% for the TR450 sample. Although the fractional free volume increased, the permeability of the TR polymer samples was much higher than in other classes of polymers, including polyimides, having similar free volume values. This higher than expected permeability may be due to a more favorable free volume distribution.

Acknowledgements

The authors would like to acknowledge ConocoPhillips and United States Department of Energy (DE-FG02-02ER15362) for

their support. A portion of this research is based upon work supported by the U.S. National Science Foundation under Grant No. DMR #0423914.

References

[1] R.W. Baker, K. Lokhandwala, Natural gas processing with membranes: an overview, Industrial and Engineering Chemistry Research 47 (2008) 2109–2121.
[2] H.B. Park, C.H. Jung, Y.M. Lee, A.J. Hill, S.J. Pas, S.T. Mudie, E. Van Wagner, B.D. Freeman, D.J. Cookson, Polymers with cavities tuned for fast selective transport of small molecules and ions, Science 318 (2007) 254–258.
[3] H.B. Park, S.H. Han, C.H. Jung, Y.M. Lee, A.J. Hill, Thermally rearranged (TR) polymer membranes for CO_2 separation, Journal of Membrane Science 359 (2010) 11–24.
[4] A.W. Thornton, K.M. Nairn, A.J. Hill, J.M. Hill, New relation between diffusion and free flume: I. Predicting gas diffusion, Journal of Membrane Science 338 (2009) 29–37.
[5] P. Alivisatos, M. Buchanan, Basic research needs for carbon capture: beyond 2020, 2010, http://science.energy.gov/~/media/bes/pdf/reports/files/CCB2020_rpt.pdf.
[6] C.H. Jung, J.E. Lee, S.H. Han, H.B. Park, Y.M. Lee, Highly permeable and selective poly(benzoxazole-co-imide) membranes for gas separation, Journal of Membrane Science 350 (2010) 301–309.
[7] C.H. Jung, Highly permeable, selective polymer membranes for gas separation, Ph.D. Thesis, Hanyang University (2008).
[8] Y. Jiang, F. Willmore, D. Sanders, Z.P. Smith, C.P. Ribeiro, C.M. Doherty, A. Thornton, A.J. Hill, B.D. Freeman, Cavity size, sorption and transport characteristics of thermally rearranged (TR) polymers, Polymer 52 (2011) 2244–2254.
[9] M. Calle, Y.M. Lee, Thermally rearranged (TR) poly(ether-benzoxazole) membranes for gas separation, Macromolecules 44 (2011) 1156–1165.
[10] S.H. Han, J.E. Lee, K.J. Lee, H.B. Park, Y.M. Lee, Highly gas permeable and microporous polybenzimidazole membrane by thermal rearrangement, Journal of Membrane Science 357 (2010) 143–151.
[11] J.I. Choi, C.H. Jung, S.H. Han, H.B. Park, Y.M. Lee, Thermally rearranged (TR) poly(benzoxazole-co-pyrrolone) membranes tuned for high gas permeability and selectivity, Journal of Membrane Science 349 (2010) 358–368.
[12] S.H. Han, N. Misdan, S. Kim, C.M. Doherty, A.J. Hill, Y.M. Lee, Thermally rearranged (TR) polybenzoxazole: effects of diverse imidization routes on physical properties and gas transport behaviors, Macromolecules 43 (2010) 7657–7667.
[13] Z.P. Smith, D.F. Sanders, C.P. Ribeiro, R. Guo, B.D. Freeman, D.R. Paul, J.E. McGrath, S. Swinnea, Gas sorption and characterization of thermally rearranged polyimides based on 3,3′-dihydroxy-4,4′-diamino-biphenyl (HAB) and 2,2′-bis-(3,4-dicarboxyphenyl) hexafluoropropane dianhydride (6FDA), Journal of Membrane Science, submitted.
[14] D. Wilson, H.D. Stenzenberger, P.M. Hergenrother, Polyimides, Chapman and Hall, New York, 1990.
[15] M.K. Ghosh, K.L. Mittal, Polyimides, Marcel Dekker Inc., New York, 1996.
[16] H.Q. Lin, B.D. Freeman, Permeation and diffusion, in: H. Czichos, T. Saito, L. Smith (Eds.), Springer Handbook for Materials Measurement Methods, Springer, 2011.
[17] H. Ohya, V.V. Kudryavtsev, S.I. Semenova, Polyimide Membranes – Applications, Fabrications, and Properties, Gordon and Breach, 1996.
[18] Standard test method for density of plastics by the density-gradient technique, in: ASTM D1505, 2010.
[19] R. Guo, D.F. Sanders, Z.P. Smith, B.D. Freeman, J.E. McGrath, Synthesis and characterization of thermally rearranged (TR) polymers: effects of ortho-positioned functional groups of polyimide precursors, in preparation.
[20] G.L. Tullos, L.J. Mathias, Unexpected thermal conversion of hydroxy-containing polyimides to polybenzoxazoles, Polymer 40 (1999) 3463–3468.
[21] G.L. Tullos, J.M. Powers, S.J. Jeskey, L.J. Mathias, Thermal conversion of hydroxy-containing imides to benzoxazoles: polymer and model compound study, Macromolecules 32 (1999) 3598–3612.
[22] P.R. Bevington, K.D. Robinson, Data Reduction and Error Analysis for the Physical Sciences, McGraw Hill, Boston, 2003.
[23] S. Matteucci, Y. Yampolskii, I. Pinnau, B.D. Freeman, Transport of gases and vapors in glassy and rubbery polymers, in: Y. Yampolskii, I. Pinnau, B.D. Freeman (Eds.), Materials Science of Membranes for Gas and Vapor Separation, John Wiley & Sons, Chichester, 2006, pp. 2–46.
[24] L.M. Robeson, Correlation of separation factor versus permeability for polymeric membranes, Journal of Membrane Science 62 (1991) 165–185.
[25] L.M. Robeson, The upper bound revisited, Journal of Membrane Science 320 (2008) 390–400.
[26] W.J. Koros, A.H. Chan, D.R. Paul, Sorption and transport of various gases In polycarbonate, Journal of Membrane Science 2 (1977) 165–190.
[27] Y. Hirayama, T. Yoshinaga, Y. Kusuki, K. Ninomiya, T. Sakakibara, T. Tamari, Relation of gas permeability with structure of aromatic polyimides I, Journal of Membrane Science 111 (1996) 169–182.
[28] J.G. Wijmans, R.W. Baker, The solution-diffusion model – a review, Journal of Membrane Science 107 (1995) 1–21.
[29] T.T. Moore, W.J. Koros, Gas sorption in polymers, molecular sieves, and mixed matrix membranes, Journal of Applied Polymer Science 104 (2007) 4053–4059.
[30] A.C. Puleo, D.R. Paul, S.S. Kelley, The effect of degree of acetylation on gas sorption and transport behavior in cellulose-acetate, Journal of Membrane Science 47 (1989) 301–332.
[31] D.Q. Vu, W.J. Koros, S.J. Miller, Mixed matrix membranes using carbon molecular sieves – I. Preparation and experimental results, Journal of Membrane Science 211 (2003) 311–334.
[32] R.W. Baker, Membrane Technology and Applications, John Wiley & Sons, Chichester, 2004.
[33] A. Bondi, van der, Waals volumes and radii, The Journal of Physical Chemistry 68 (1964) 441–451.
[34] A. Bondi, Physical Properties of Molecular Crystals, Liquids, and Glasses, Wiley, 1968.
[35] W. Xie, H. Ju, G. Geise, B.D. Freeman, J.I. Mardel, A.J. Hill, J.E. McGrath, Effect of free volume on water and salt transport properties in directly copolymerized disulfonated poly(arylene ether sulfone) random copolymers, Macromolecules 44 (2011) 4428–4430.
[36] B.W. Rowe, B.D. Freeman, D.R. Paul, Effect of sorbed water and temperature on the optical properties and density of thin glassy polymer films on a silicon substrate, Macromolecules 40 (2007) 2806–2813.
[37] D.W. van Krevelen, Properties of Polymers, Elsevier Publ. Comp., 1972.
[38] J.Y. Park, D.R. Paul, Correlation and prediction of gas permeability in glassy polymer membrane materials via modified free volume based group contribution method, Journal of Membrane Science 125 (1997) 23–39.